

Novel Functional Nitrile Butadiene Rubber/Magnetite Nano Composites for NTCR Thermistors Application

Salih S. Al-Juaid,¹ E. H. El-Mossalamy,¹ H. M. Arafa,² A. A. Al-Ghamdi,³ A. M. Abdel Daiem,^{3,4} Farid El-Tantawy⁵

¹Faculty of Science, Department of Chemistry, King Abdulaziz University, Jeddah 21569, Kingdom of Saudi Arabia

²Faculty of Science, Department of Chemistry, University of Tabuk, Tabuk, Kingdom of Saudi Arabia

³Faculty of Science, Department of Physics, King Abdulaziz University, Jeddah 21569, Kingdom of Saudi Arabia

⁴Faculty of Science, Department of Physics, Zagazig University, Zagazig, Egypt

⁵Faculty of Science, Department of Physics, Suez Canal University, Ismailia, Egypt

Received 4 November 2010; accepted 12 January 2011

DOI 10.1002/app.34158

Published online 12 April 2011 in Wiley Online Library (wileyonlinelibrary.com).

ABSTRACT: A new negative temperature coefficient of resistor (NTCR) thermistors based on nitrile butadiene rubber/magnetite (NBR/Fe₃O₄) nanocomposites were successfully fabricated by conventional roll milling technique. X-ray diffraction and transmission (TEM) analysis showed that the product is mainly magnetite nanoparticles with diameter of 10–13 nm. The microstructure of (NBR/Fe₃O₄) nanocomposites were examined by scanning electron microscopy (SEM) and FTIR spectroscopy. The dispersion of magnetite nanoparticles in the NBR rubber matrix and interfacial bonding between them were rather good. The thermal stability of nanocomposites was also obviously improved with the inclusion of the magnetite nanoparticles. The thermal conductivity, thermal diffusivity and specific heat of nanocomposites were investigated. The

electrical conductivity of the NBR/Fe₃O₄ increases with the rise in temperature exhibiting a typical negative temperature coefficient of resistance (NTCR) behavior like a semiconductor. The nature of the temperature variation of electrical conductivity and values of activation and hopping energy, suggest that the transport conduction process is controlled by hopping mechanism. Values of characteristics parameters of the thermistors like thermistor constant, thermistor sensitivity and thermistor stability is quite good for practical application as NTCR devices at high temperature. © 2011 Wiley Periodicals, Inc. *J Appl Polym Sci* 121: 3604–3612, 2011

Key words: NBR rubber; magnetite nanoparticles; network structure; electrical and thermal properties

INTRODUCTION

Electrically conductive polymer nanocomposites have attracted a great deal of scientific and commercial interest.^{1,2} These conductive nanocomposites have been widely used in newer areas and for various applications such as touch control switches,³ electromagnetic interference shielding,^{1,2} floor heating,⁴ electrostatic discharge protection,⁵ corrosion-protection,⁶ PTCR thermistors,² temperature sensors,⁷ gas sensors,⁸ magnetic sensors,⁹ piezoresistive sensors,¹⁰ etc. One of the important methods to form a charge carrier path in an insulating polymer matrix is the incorporation of conductive additives like carbon black,¹¹ carbon fiber,¹² carbon nanotubes,¹³ graphite,¹⁴ metal,¹⁵ metal oxide,¹⁶ conducting organic polymer^{17–20} and others. Nanometer sized iron oxides such as magnetite (Fe₃O₄) and/or maghemite

(Fe₂O₃) possess magnetic, catalytic, conducting and biological properties and are suitable for applications in cell separation, protein purification, targeted drug delivery, environmental and food analyses, organic and biochemical synthesis, and industrial water treatment.^{11–16} Magnetic nanoparticles embedded in polymer matrixes have excellent potential for electromagnetic device applications like electromagnetic interference (EMI) noise reduction.^{18–21} Recently these conductive composite materials have been very popular due to their low attractive costs, high flexibility, and weather and chemical resistant properties. However, negative temperature coefficient of resistance (NTCR) thermistors are semiconductor materials and are found in an ever-increasing number of electrical and electronic devices since the 1940s in telecommunication circuit compensation.^{1,13} An important thermal-sensitive feature of conducting polymer composites, that is, the resistivity decreases with increasing temperature, which is also known as NTCR effect.^{14,15} They are widely used in various industrial and domestic applications, for examples, elements for the suppression on in-rush current, for temperature measurement and control,

Correspondence to: F. El-Tantawy (faridtantawy@yahoo.com).

and for compensation for other circuit elements.^{6,10} In general, knowing physical properties of the rubber nanocomposites has gained significant importance in the design of new systems. The temperature fields in composite materials cannot be determined unless the thermal properties such as thermal conductivity, specific heat of the media are known and is crucial in a number of industrial processes.^{8,12} With the above consideration in mind, the aim of this study is to fabricate a new nanoconducting composites contains nitrile butadiene rubber (NBR) as rubber matrix reinforced magnetite nanoparticles for NTCR thermistors applications. The effect of magnetite content on the network structure and thermal stability of composites were investigated in details. The applicability of NBR/magnetite nanocomposites as NTCR thermistors were tested, too.

EXPERIMENTAL PROCEDURES

Synthesis of magnetite (Fe₃O₄) nanoparticles

The synthesis was carried out according to the following procedure: 0.025 mol of FeCl₂·4H₂O was dissolved in 100 mL deionized water in a 1000 mL round bottom flask, with magnetic stirring at room temperature for 30 min. Then, 7 mol ammonia (Conc. 15%) in 100 mL deionized water was poured into the above ferrous chloride solution at a rate of 1 cm³/sec until pH becomes 10 under vigorous stirring. The mixture was aged at 80°C for 8 h under stirring, the precipitate was centrifuged and then dried at 70°C for 24 h. The dried material was washed by Soxhlet extraction over ethanol for 24 h, and then dried overnight at room temperature in air. Calcination was performed at 300°C for 3 h in a furnace.

Preparation of the NBR/magnetite nanocomposites

NBR in this study was a commercial grade purchased from Alexandria Trade Rubber Co. (Alexandria, Egypt), with density 0.98 g/cm³, acrylonitrile content = 34%; Mooney viscosity ML (1 + 4) at 100°C = 45 + 5 (ASTM D 1646); Average molecular weight = 163,376; glass temperature of about -36°C. The composites of NBR with magnetite nanoparticles were prepared in ratios of 100/0, 90/05, 90/10, 85/15, and 80/20 (wt %) and are designated F0, F5, F10, F15, and F20, respectively, where the numbers indicate the weight percentages of Fe₃O₄ in the composites. The formulation of the NBR composites used in experiments is shown in Table I. The physical mixing of the NBR/Fe₃O₄ composites was carried out with an open two-roll mill (150 × 300 mm²) at room temperature at a rotor speed of 60 rpm and the nip gap of about 1 mm. Subsequently, the other

TABLE 1
Formulation Used for the Preparation of the Nanocomposites

Sample ingredients	F0	F5	F10	F15	F20
NBR	100	100	100	100	100
Fe ₃ O ₄	0	5	10	15	20
Stearic acid	3	3	3	3	3
Zinc oxide	4	4	4	4	4
DOP ^a	1	1	1	1	1
MBTS ^b	2	2	2	2	2
TMTD ^c	1	1	1	1	1
PBN ^d	1	1	1	1	1
Sulfur	2	2	2	2	2

All values are expressed as (phr) by weight.

^a Dioctyle phthalate.

^b MBTS is dibenzthiazyl disulphide.

^c Tetra methyl thiuram disulfide

^d PBN is phenyl-β-naphthyl-amine.

ingredients including vulcanizing agent were added to the composite during the roll-mixing process according to the standard compounding procedures. The mixed compound was preheated for 30 min and vulcanized for 1 h at 153° under a pressure of 500 KN/m².

Characterization and test

X-ray diffraction

Powder X-ray diffraction patterns of as prepared magnetite nanoparticles were recorded at room temperature on Rigaku Miniflex with Cu Kα radiation (λ = 0.154 nm) at 20 kV and 15 mA. The spectra of the powder were scanned over the range of 50 to 700 (2θ), with a step rate of 0.02° (2θ) and a fixed counting time of 10 s for each step, to obtain spectra with sufficient signal-to-noise ratio.

Transmission and scanning electron microscopy

Transmission electron photographs of as prepared magnetite nanoparticles were obtained from Philips CM 12 transmission electron microscope (TEM) with an accelerating voltage 50 KV. Scanning electron microscopy (SEM) was used to investigate the surface morphology/microstructure of the as prepared Fe₃O₄ and NBR composites after the vulcanization process. Surfaces of the test samples were carefully cut, mounted on a SEM stub using double-sided carbon tape, and then examined under an electron microscope (model JSM-5310, JEOL, Tokyo, Japan).

Fourier transformed infrared analysis

The Fourier transformed infrared (FTIR) spectroscopy of the samples were determined using FT-IR 1750 (Perkin-Elmer Instruments), utilizing potassium

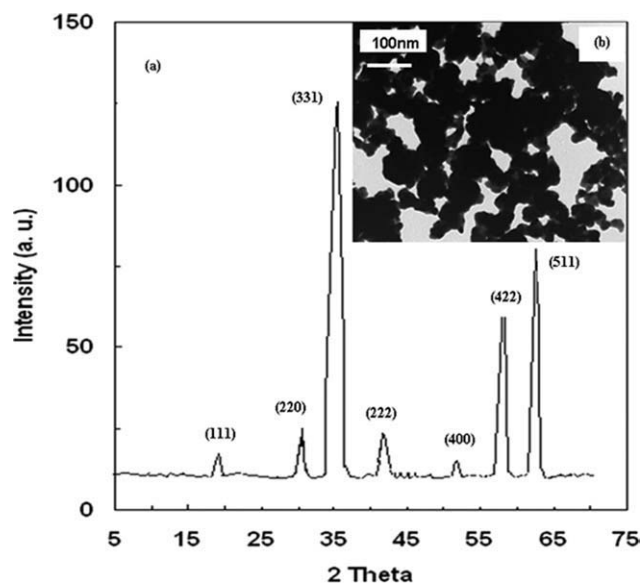


Figure 1 (a) XRD pattern of as prepared magnetite nanoparticles and (b) Transmission electron microscopy (TEM) of the as prepared magnetite.

bromide (KBr, spectroscopic grade) pellets. The spectrum was measured and recorded in the wave number range of 500–4000 cm^{-1} .

Thermogravimetric study

Thermal stability of neat NBR and NBR/magnetite nanocomposites was observed by thermogravimetric analysis (TGA) with Shimadzu TGA-50H thermogravimetric analyzer and thermogravimetric parameters were determined using the associated TGA-50H software. The heating ramp of 10°C/min under air flow, from room temperature up to 600°C.

Dynamic electrical conductivity

To check the effect of temperature on the electrical conductivity as special type of two probe (positive and negative electrode) sample holder fitted in a controlled heating chamber was used and the current was measured using a Multi-Mega-Ohmmeter type MOM12 (from WTW Co., Germany). The data were automatically collected using a suitable interface and data acquisition pc code. The side of samples were covered by silver paste to ensure electrical contact. The temperature sweep range was from room temperature 20 to 200°C.

Thermal properties

Thermal properties such as thermal conductivity, thermal diffusivity, specific heat capacity, and glass transition temperature of green NBR matrix and NBR/magnetite nanocomposite were measured

using a differential scanning calorimetry (DSC) instrument (SETARAM DSC-131). Indium was used as a reference material for the calibration of the instrument. DSC measurements were performed at 5°C/min heating rate.

RESULTS AND DISCUSSION

Structure analysis of magnetite and nanocomposites

Figure 1(a) shows the X-ray diffraction pattern of as prepared magnetite (Fe_3O_4) nanoparticles. All peaks of magnetite can be assigned to the cubic structure of magnetite and match well with those of magnetite (ICSD-No. 88-0315). It is clear that the particles were highly crystallized in a cubic structure.¹⁵ The calculated lattice parameter by least square fit is $a = 8.378 \text{ \AA}$. The average particle size of magnetite calculated by using Scherrer formula is about 12 nm. The typical TEM of the as-synthesized magnetite is depicted as inset in Figure 1(b). The TEM studies indicate that the powder particles were of nanometer size. They are approximately spherical in shape and in the range 10–13 nm matching well those obtained from X-ray.

SEM image of as prepared nano magnetite is shown in Figure 2. It is seen that magnetite particles are spherical with diameters in the range of 12 and 15 nm and are polydisperse. Furthermore, few of the magnetite particles are found to be aggregated owing to the magnetodipole interactions between the particles.^{12,13}

Figure 3(a,b) presents the SEM of the NBR/magnetite nanocomposites samples F5 and F20, respectively. In Figure 3(a), the micrograph indicates the

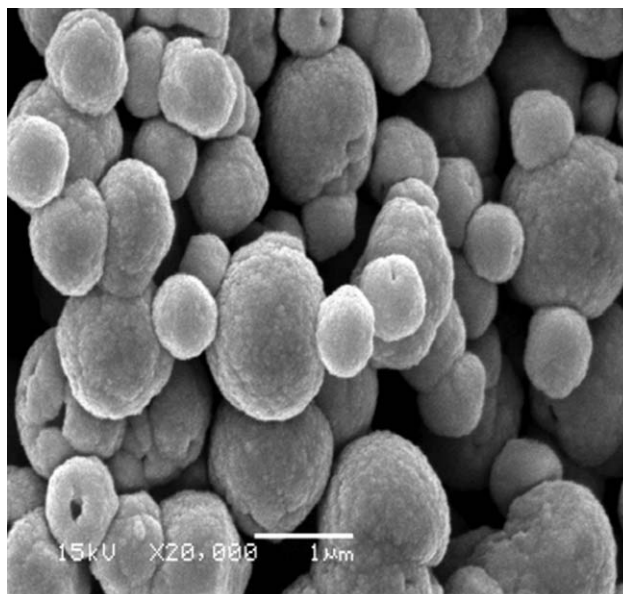


Figure 2 SEM image of as prepared magnetite nanoparticles.

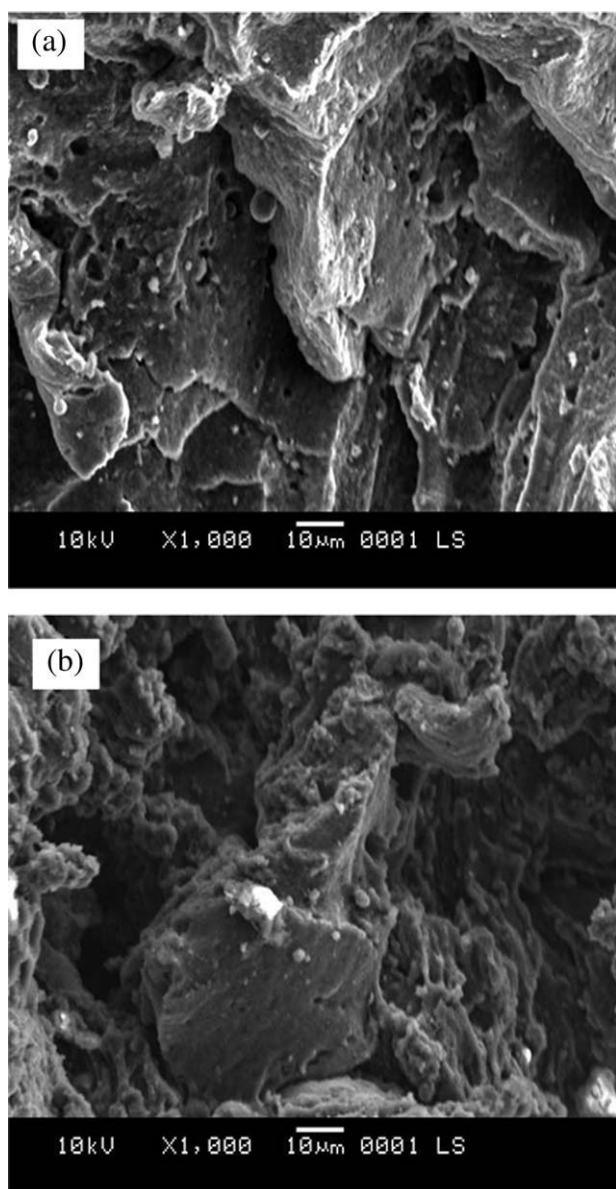


Figure 3 (a) Scanning electron micrograph of the NBR/magnetite nanocomposites of samples F5. (b) Scanning electron micrograph of the NBR/magnetite nanocomposites of sample F20.

existence of magnetite nanoparticles with a certain degree of porosity into composites. SEM image for Fe20 sample [Fig. 3(b)] shows the presence of spherical magnetite nanoparticles, dispersed homogeneously within the NBR polymer matrix and located in the interfacial regions between NBR particles. There are spots that show diffusing of magnetite nanoparticles into the NBR matrix. In addition, at the interfacial zones, good contacts exist among the NBR matrix elastomer and the magnetite nanoparticles, forming a network of magnetite conductive paths. These findings confirm the morphology enhances with inclusion magnetite nanoparticles into NBR matrix.

To give further evidence for magnetite nanoparticles enhances the network structure of nanocomposites, cross linking density (CLD), extent of filler reinforcement (EFR) and interparticle distance (IPD) were measured. The CLD of vulcanized samples were measured from equilibrium swelling methods on the basis of the Flory–Rehner eqs. (7) and (11). The thickness and weight of sample used were about 1.5 mm and 1.0 g, respectively. The sample was immersed in 100 mL of toluene in the dark for 48 h at room temperature. The CLD and/or the number of active network chain segments per unit of volume is defined as^{8,9}:

$$CLD = -[\ln(1 - \phi_r) + \phi_r + \chi\phi_r^2]/V_0 \left(\phi_r^{1/3} - \frac{\phi_r}{2} \right) \quad (1)$$

where V_0 is the molar volume of the solvent (106.2 cm³ for toluene), and χ is the Flory–Huggins polymer–solvent interaction index. The value of χ for toluene is 0.393.17 and ϕ_r is the volume fraction of the NBR rubber in the swollen mass and is given by^{9,10,21}:

$$\phi_r = \frac{\omega_2/\rho_2}{\omega_2/\rho_2 + (\omega_1 - \omega_2)/\rho_1} \quad (2)$$

where ω_1 and ω_2 are the weights of the swollen and deswollen samples, respectively, and ρ_1 and ρ_2 are the densities of the solvent and NBR polymer matrix, respectively.

The IPD is defined by^{11,12}:

$$IPD = -D \left[\left(\frac{k\pi}{6v} \right)^{1/3} - 1 \right] \quad (3)$$

where D is the magnetite particle diameter, $k = 1$ (for cubic packing) and v is the volume fraction of rubber network and is given by¹³:

$$\left(\frac{1}{v} \right) = 1 + \left(\frac{\omega_3\rho_2}{\omega_0\rho_1} \right) \quad (4)$$

where ω_0 is the weight of neat sample and ω_3 is weight of absorbed solvent.

The EFR can be expressed as^{6,14}:

$$EFR = \left(\frac{v}{v_{r0}} \right) / \left(\frac{\beta}{1 - \beta} \right) \quad (5)$$

where v_{r0} is the volume fraction of rubber in the filled vulcanizate and β is the content of magnetite.

The estimated values of CLD, EFR, and IPD as a function of magnetite content into nanocomposites is depicted in Figure 4. One can clearly see that the CLD and EFR of the composites increased while IPD decreased with increasing magnetite nanoparticles

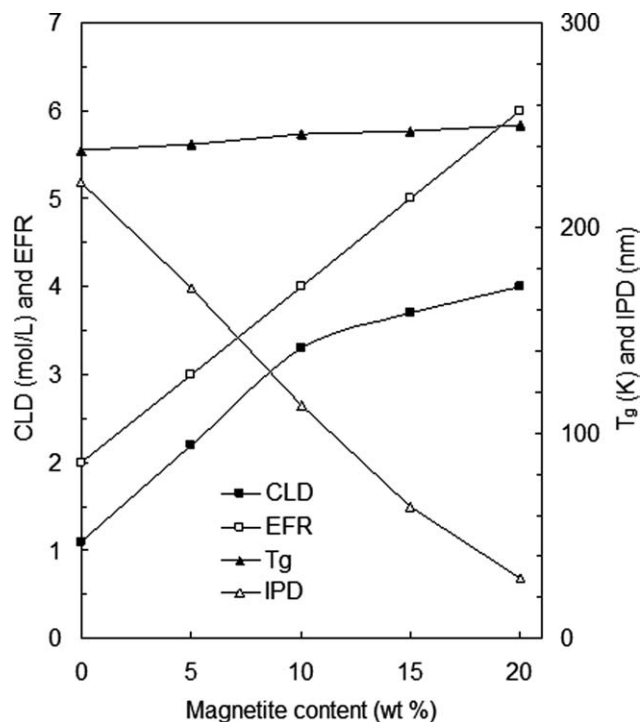


Figure 4 CLD, EFR, IPD, and glass transition temperature (T_g) as a function of magnetite content of NBR/magnetite composites.

content. The increase of CLD may be apparently due to the increase of the number of elastically effective chains with magnetite loading into NBR composites.

The EFR of composites increased with increasing in conductive magnetite content as shown in Figure 4. The degree of reinforcement achieved by incorporation of magnetite nanoparticles was due to good adhesion between magnetite nanoparticles and NBR elastomer matrix, which will lead to the better electrical and thermal properties of composites. On the other hand, the IPD decreased with increasing magnetite nanoparticles content into composites. This is due to the fact that, with increasing magnetite loading the number of voids at the interface decreases and the interface bonding increases. This result once again supported that, in the NBR/magnetite nanocomposites, the interaction between NBR polar matrix and magnetite nanoparticles was very strong, and the dispersion of magnetite in the matrix was very fine. The fine dispersion of magnetite at high magnetite loading in return approved strong interaction between magnetite and NBR matrix.

Glass transition temperature (T_g) is another indicative of interfacial bonding between filler and matrix. An increase in T_g with increase in magnetite content is observed for NBR nanocomposites in Figure 4. This increase in T_g is attributed to an increase in molecular texturing with increase in magnetite content into composites, which enhances the molecular motions of the conductive site, leading to higher T_g .

This might be also attributed to the free volume decrease as a result of restriction of the chain packing due to the increase of the CLD and interracial adhesion of the NBR chains and magnetite nanoparticles as confirmed above.^{1,15}

Accordingly, the FTIR spectra experiment of prepared magnetite, neat NBR and NBR/magnetite nanocomposites was done to prove the reaction between magnetite nanoparticles and NBR polymer matrix, as shown in Figure 5. The FT-IR spectra presented in this figure, the absorption peaks at 1400 and 1632 cm^{-1} belongs to the stretching vibration mode of Fe–O bonds in magnetite, which tally with the published results.^{3,5} The bands at 1981 and 2160 cm^{-1} indicated stretching of CH_2 and CH_3 groups in NBR matrix. In addition, the peaks appears at 2844 and 2920 cm^{-1} is attributed to the stretching vibration of NBR segment, which is assigned to CH_2 and CH_3 adsorbed by magnetite nanoparticles and the interaction among magnetite and NBR chains.¹⁸ This strong clue that the NBR segments were successfully linked onto the magnetite nanoparticles surface.

Thermal stability of nanocomposites

To understand thermal stability of the NBR/magnetite nanocomposites and specially to find application at high temperature, TGA analysis has been carried out. Thermal stability of NBR and NBR/magnetite

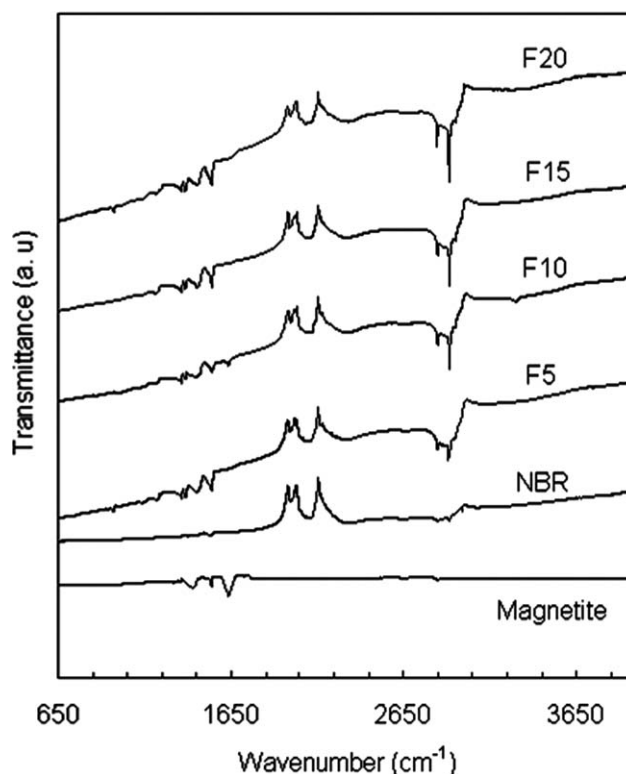


Figure 5 FTIR spectroscopy of prepared magnetite and NBR/magnetite nanocomposites.

nanocomposites is plotted in Figure 6. It is seen that, a shift of rapid degradation region towards higher temperature can be seen for NBR after adding the magnetite's nanoparticles. Figure 5 reveals two main weight losses. The first occurred at 127°C and corresponds to loss of moisture.^{16,18} The second degradation step is observed as a continuous weight loss starting at ca. 348, 335, 323, 312, and 299°C for NBR, Fe5, Fe10, Fe15, and Fe20, respectively, relating to the decomposition of the respective conducting polymer backbone and magnetite. Meanwhile, the weight loss of NBR/magnetite nanocomposites at the same temperature is the smallest among all studied specimens. The reason is that magnetite's can impose the restriction on the mobilization of NBR rubber macromolecules and conduct heat homogeneously and avoid the heat concentration.^{4,5} Therefore, the thermal stability of NBR was further improved by adding magnetite nanoparticles compared to neat NBR. Our result indicates that the composites is having better thermal stability due homogenous dispersion and good interface adhesion of magnetite into NBR matrix. This in agreement with the discussions mentioned earlier.

Thermal properties studies

Known that thermal conductivity, thermal diffusivity and specific heat capacity of the nano composites has gained significant importance in the design of new systems and are crucial in a number of industrial processes.¹² Thermal conductivity (K_c), Thermal diffusivity (K_d) and specific heat capacity (C_p) of NBR/magnetite nanocomposites as a function of magnetite content is depicted in Figure 7. In comparison with neat NBR, the composites show prominent improvement of K_c and C_p under lower magnetite content, and the highest K_c of nanocomposites (appears at 20 wt% of magnetite content) is about three times higher than that of neat NBR rubber matrix. It is clear K_d increased with increasing magnetite content into nanocomposites. At low magnetite content both K_c and K_d increases slightly of composites. This is attributed to a few magnetite nanoparticles contribute to form conductive chains, and the NBR matrix is almost continuous.⁹⁻¹² With increasing magnetite content, many magnetite nanoparticles touch each other and the number of effective conductive chains density increasing, which greatly contribute to the higher both K_c and K_d of NBR/magnetite composites.^{17,18} This indicates that the heat conduction property of NBR composites are enhances with increasing magnetite nanoparticles content into composites. Furthermore, we believe that the uniform distribution and intergrain contacts of the magnetite nanoparticles in the NBR matrix is benefi-

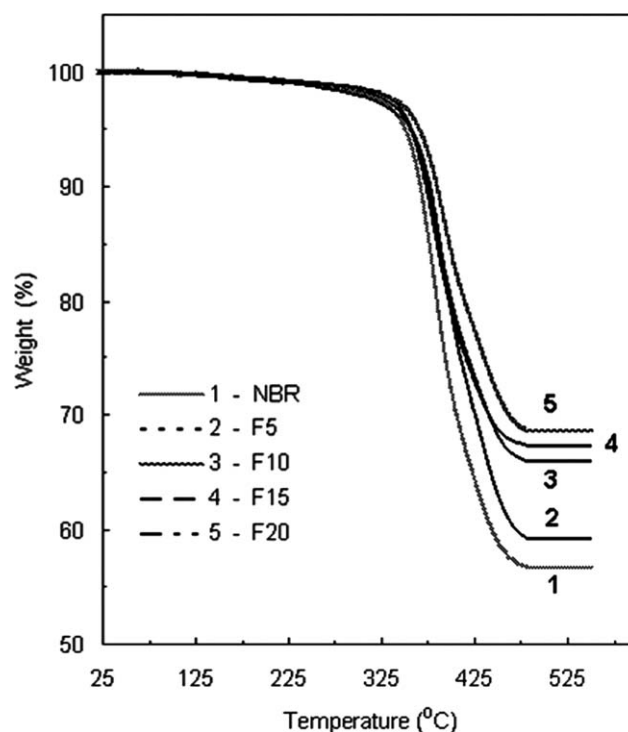


Figure 6 TGA curve of neat NBR and NBR/magnetite nanocomposites.

cial to improve the heat insulation property of the composite systems at high magnetite content.

The thermal conductivity can be predicted theoretically utilizing Agari model as follows^{8,9}:

$$\log K_c = V_F C_2 \log K_F + V_P \log(C_1 K_P) \quad (6)$$

where K_F and K_P are the thermal conductivities of magnetite and NBR elastomer matrix, respectively, V_F and V_P are the volume fraction of magnetite and NBR matrix, respectively and C_1 is related with the crystallinity of the NBR matrix, and C_2 presents the ease for the formation of conductive chains.⁸ The values of C_1 and C_2 should be between 0 and 1. The closer C_2 values are to 1, the more easily conductive chains are formed in the composite. The experimental data are well-fitted into the Agari model as shown in Figure 7. A possible explanation is that the ease for the formation of conductive chains was taken into account in the Agari model.⁸

However, the increase in the specific heat of nanocomposites with the increase of magnetite contents as shown in Figure 7, could be due to greater stability of thermal conductive paths and good interface between filler and matrix and consequently reducing phonon scattering. The interfacial area can be viewed as a stable structure since the conductive particles are well connected at the interface, and become more effective to form heat conduction "net bridges" to transfer heat through the sample, and

this usually causes reduced diffusive of scattering phonons. In addition, the specific heat of NBR composites with 20 wt % had a satisfying specific heat capacity for NTCR thermistor applications.²⁰

Applicability of nanocomposites as NTCR thermistors

It is well known that the NTCR composite thermistors, for their unique property, are much interesting in various applications in sensing devices; therefore, not surprisingly, they constitute an important business segment for most electro composite manufacturers.^{1,15} The key material property relevant for thermistor applications is the electrical conductivity versus temperature ($\sigma - T$) behavior. The variation of electrical conductivity with temperature for NBR/magnetite nanocomposites is depicted in Figure 8. The electrical conductivity data of the composites reveal that they are semiconducting in nature. It is observed that the values of electrical conductivity increased as the magnetite content increase into composites. Since, the grains are much larger in size and the grain surface area is much smaller. This enhancement of density and intergrain contacts leads to higher electrical conductivity in the nanocomposite. The electrical conductivity increases by about three orders when the ambient temperature increases from room temperature to 200°C. It is seen that the electrical conductivity increases with increasing temperature and the composites behave as a NTCR thermistors. In addition, it is worthily to note that an enhanced negative temperature coefficient of resistivity with increasing magnetite nanoparticles content into composites was observed. The increase of electrical conductivity with temperature is evoked mainly to four reasons: the first is the thermal emission of charge carriers via the width between neighboring magnetite particles when the nanoparticles are separated by a gap but not equivalent to physical link.¹ The second is that the reordering of magnetite nanoparticles takes place during heating; leading to formation of new conducting paths. This will enhances the driving force of charge carriers transport and process of conduction, thereof the conductivity increases.^{2,3} The third is during heating; some sort of oxidative cross linking at the surface takes place, which enhances electrical conductivity. The fourth might be due to the compensation effect of magnetite nanoparticles in the interface (i.e. semiconducting phases), which results in a lowered highest potential barrier.^{4,5} As shown in Figure 8, it is interesting to note that a nearly linear relationship is obtained between the logarithmic values of electrical conductivity and the temperature for nanocomposites, an indication of good NTCR thermistor characteristic.

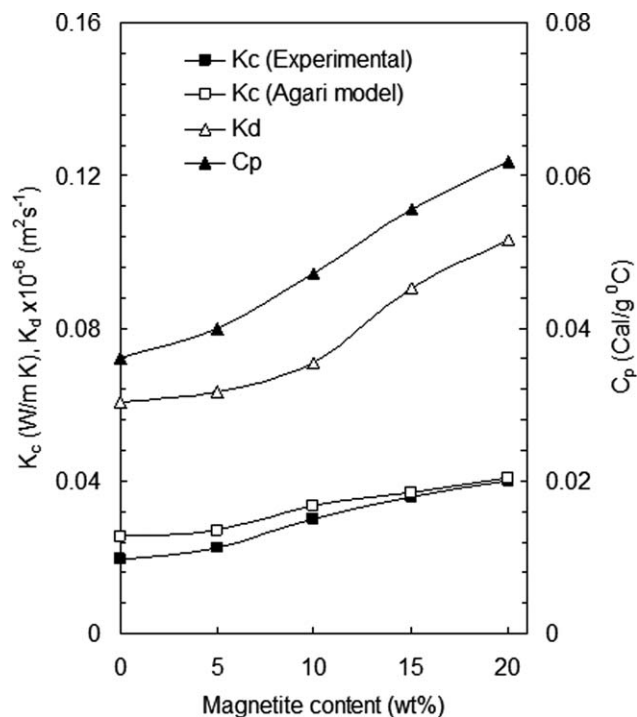


Figure 7 Thermal conductivity (K_c), Thermal diffusivity (K_d) and specific heat capacity (C_p) of NBR/magnetite nanocomposites.

To investigate the mechanism of charge carriers transport in the NBR/magnetite nanocomposites, the activation and hopping energies have been estimated. As the barrier – layer electrical conductivity depends on the activation energy (E_a) required to surmount the potential barrier, the electrical conductivity (σ) of the composites is given by the following equation^{6,7}:

$$\sigma = \sigma_0 \exp(-E_a/KT) \quad (7)$$

And the hopping energy (E_h) is given by the following formula³:

$$\sigma\sqrt{T} = \sigma_0 \exp(-E_h/KT) \quad (8)$$

where σ_0 it is the electrical conductivity at infinite temperature (approximately independent on the temperature), K is Boltzmann's constant and T is the Kelvin temperature.

The estimated values of both the E_a and E_h as a function of magnetite content is plotted in Figure 9, and are calculated from the slopes of the plots in the temperature range of 20 to 200°C. It is seen that both the E_a and E_h decreases with magnetite rising into NBR/magnetite nanocomposites. This can be explained by considering that the increasing of magnetite content causes stronger carriers interaction governing the band width between conductive sites.

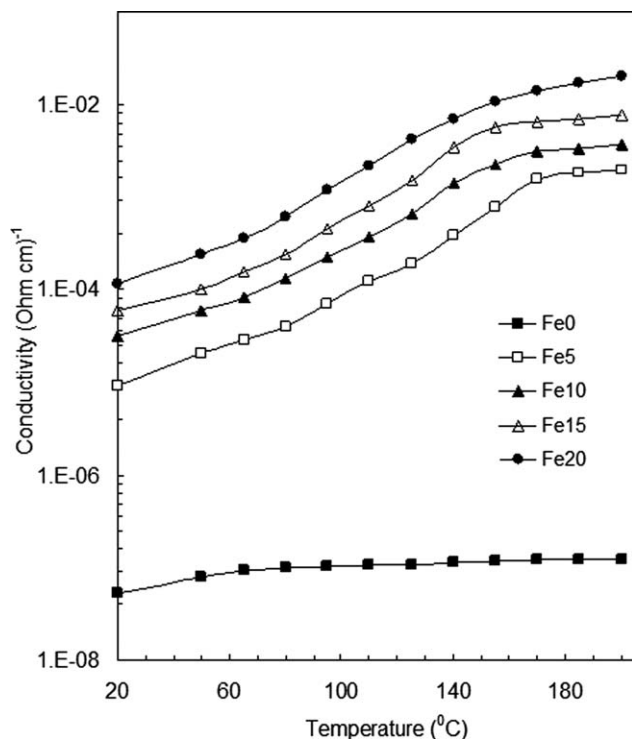


Figure 8 Variation of electrical conductivity with temperature for NBR/Fe₃O₄ nanocomposites.

As a result, the energy required to liberate a free charge carrier is reduced.^{3,8} It is worthily to mention that the values of E_a is far from the value of E_h in nanocomposites. This is strong clue that the conduction mechanism of conductivity of NBR/magnetite nanocomposites is controlled by hopping conduction.^{1,2}

The thermistor constant (B) the thermistor sensitivity (α) and stability factor (SF), which are the most important characteristics of technical interest for NTCR thermistors. The B , which is a measure of the sensitivity of the device over a given temperature of the composites and is given by expression^{10,12}:

$$B = \frac{\ln \rho_2 - \ln \rho_1}{1/T_2 - 1/T_1} \quad (9)$$

where ρ_1 and ρ_2 are the resistivities measured at temperature $T_1(25^\circ\text{C})$ and $T_2(100^\circ\text{C})$, respectively.

The α is defined by the temperature coefficient of conductivity, which can be expressed as a function of the B parameter, according to the following formula¹⁴:

$$\alpha = \pm \frac{1}{\sigma} \left(\frac{d\sigma}{dT} \right) = -\frac{B}{T^2} \quad (10)$$

The stability factor (SF) is given by the following formula⁹:

$$SF = \log \left(\frac{\rho_2}{\rho_1} \right) \quad (11)$$

The computed values of B , α , and SF in the test temperature range of 20 to 100°C as a function of magnetite content of composites are plotted in Figure 9. It is clear that B increases with increasing magnetite content into NBR composites. This is attributed to the increase of the interfacial polarization and the decreases of the activation energy at the interface between magnetite and NBR matrix.¹ On the basis of the electrical properties for the NBR/magnetite NTCR thermistors, it is clear that the values of B are adjustable to desired values, dependent on the magnetite content into nanocomposites. It is interesting to note that the highest values of B for the composites, which is deemed useful for NTCR thermistors applications at high temperature.

In Figure 9, it is observed that the SF increases with increasing magnetite content into composites. This is mainly due to the stability of network structure and high crosslinking density. In Figure 9, it is seen that the α increases with increasing magnetite content into composites. This phenomena can be explained based on the microstructure of NBR composites, as the magnetite content increases the chain connectivity increases, thereat α increases. This reflect that the skeleton of the molecular structural and thermal stability enhances entire NBR composites with inclusion magnetite nanoparticles as

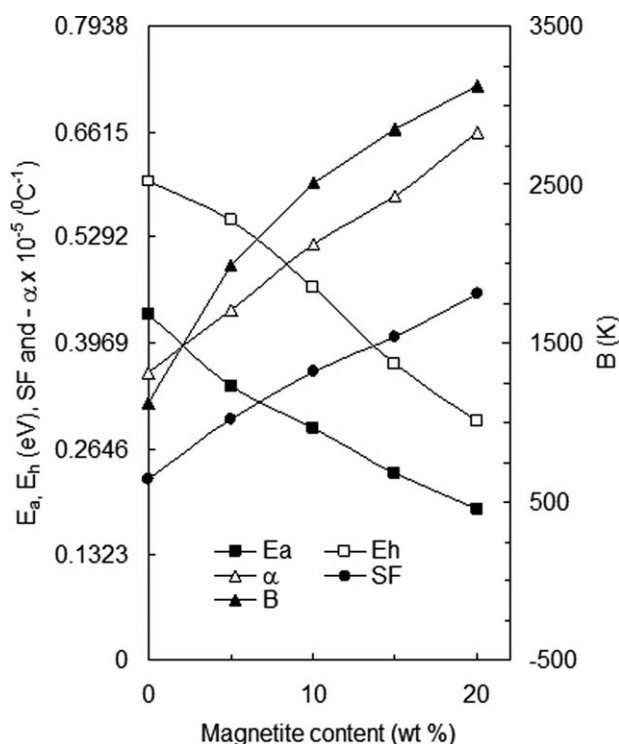


Figure 9 The computed value of E_a , E_h , B , α , and SF as a function of magnetite content of composites.

confirmed by TGA spectra and SEM images above. Finally, these thermistors materials offer a great deal of flexibility in tailoring electrical properties, depending on the magnetite loading level into composites. We propose that the NBR/magnetite nanocomposites are suitable for a wide range of applications and low cost of manufacturing of the NTCR thermistors.

CONCLUSIONS

The NTCR thermistors characteristics of NBR reinforced magnetite nanoparticles have been presented. To check the applicability of NBR/magnetite nanocomposites as NTCR thermistors, the temperature dependence of electrical conductivity of the nanocomposites were measured. Furthermore, the characteristics parameters of NTCR of thermistors such as thermistor constant, thermistor sensitivity and stability factor were estimated as a function of magnetite content. The findings of the present experimental study can be summarized as follows:

1. SEM image reveal a uniform distribution of magnetite nanoparticles into NBR matrix. The thermal stability of nanocomposites is notably improved compared to neat NBR. The NBR nanocomposites reinforced with the magnetite nanoparticles exhibited excellent overall performance improvements due to the reinforcement effect of the high surface area and interface adhesion functionalized magnetite.
2. The inclusion of magnetite nanoparticles into NBR matrix is fairly effective in achieving stable structure and enhances the thermal properties.
3. The bulk electrical conductivity increases with increasing temperature and behave as a NTCR thermistors. The $\sigma - T$ measurement of composites samples indicates the values of activation and hopping energy and the conduction mechanism of conductivity is controlled by hopping mechanism. The NBR/magnetite nanocomposites showed very good thermistor characteristics with good thermistor constant, thermistor

sensitivity and stability factor for the temperature range 25 to 100°C.

4. This finding makes the potential for expanded future industrial applications in bulk scenarios through a facile technique which improves the industrial processing, a requirement for high quality industrial-scale production of NTCR devices.

The Investigators are grateful to King Abdul Aziz University, Jeddah, Kingdom of Saudi Arabia for providing financial support for the Project No. 3-102/ 430 work.

References

1. El-Tantawy, F.; Al-Ghamdi, A. A.; Abdel Aal, N. *J Appl Polym Sci* 2010, 115, 817.
2. El-Tantawy, F.; Abdel Aal, N.; Al-Ghamdi, A. A.; El-Mossalamy, E. H. *Polym Eng Sci* 2009, 49, 592.
3. El-Tantawy, F.; Todorova, Z.; Dishovsky, N.; Dimitrov, R. *J Appl Polym Sci* 2007, 103, 2158.
4. Sau, K. P.; Chaki, T. K.; Khastgir, D. *J Appl Polym Sci* 1999, 71, 887.
5. Yan, X.; Xu, G. *Physica B: Condensed Matter* 2009, 404, 2377.
6. Arsalani, N.; Fattahi, H.; Nazarpour, M. *eXPRESS Polym Lett* 2010, 4, 329.
7. Reddy, K. R.; Lee, K. P.; Gopalan, A. I. *J Appl Polym Sci* 2007, 106, 1181.
8. Reddy, K. R.; Jeong, H. M.; Lee, Y. *J Polym Sci Part A: Polym Chem* 2010, 48, 1477.
9. Luo, Y.; Li, X.; Liu, X. *Adv Mater Sci Eng Article ID* 383842, 2009, 4, 14.
10. Yuan, C.; Liu, X.; Yang, Y.; Zho, C. *J Mater Sci* 2010, 45, 2681.
11. Sar, A.; Karaipekli, A. *Appl Therm Eng* 2007, 27, 1271.
12. Kumlutas, D.; Tavmana, I. H.; Coban, M. T. *Comp Sci Technol* 2003, 63, 113.
13. Wanga, M.; Kang, Q.; Pan, N. *Appl Therm Eng* 2009, 29, 418.
14. Mu, Q.; Feng, S.; Diao, G. *Polymer Comp* 2007, 28, 125.
15. Zhou, W.-Y.; Qi, S.-H.; Zhao, H.-Z.; Liu, N.-L. *Polym Comp* 2007, 28, 23.
16. Nie, Y.; Huang, G.; Qu, L.; Zhang, P.; Weng, G.; Wu, J. *J Appl Polym Sci* 2010, 115, 99.
17. Deepa, M.; Rao, P. P.; Sumi, S.; Radhakrishnan, A. N. P.; Koshy, P. *J Am Ceram Soc* 2010, 93, 1576.
18. Feteira, A. *J Am Ceram Soc* 2009, 92, 967.
19. Ryu, J.; Kim, K.-Y.; Choi, J.-J.; Hahn, B.-D.; Yoon, W.-H.; Lee, B.-K.; Park, D.-S.; Park, C. *J Am Ceram Soc* 2009, 92, 3084.
20. Park, K.; Yun, S. T. *J Mater Sci Mater Electron* 2004, 15, 359.
21. El-Tantawy, F.; Dishovsky, N. *J Appl Polym Sci* 2004, 91, 2756.